Good Nonlinear Figures of Merit of Au/Ag_2Se Core/Shell Nanostructures with Small Size

Xiao-Li Liu[a,*], Shuo Han[a] and Guang-Lan Sun[b]

[a] *Shandong Provincial Key Laboratory of Laser Polarization and Information Technology, Department of Physics, Qufu Normal University, Qufu 273165, China*
[b] *Basic Science Section, North China Institute of Aerospace Engineering, Langfang 065000, China*

Received: 01.04.2019 & Accepted: 06.05.2020

Doi: 10.12693/APhysPolA.138.364 *e-mail: xiaoliliu_opt@126.com

The small sized Au/Ag_2Se core/shell nanoparticles are synthesized in the organic environment. This nanostructure has a good nonlinear figures of merit. The changes of the plasmon absorption peak of the samples are obtained by UV-Vis spectrophotometer. The Au/Ag_2Se core/shell nanoparticles exhibit fascinating nonlinear optical properties which are studied by using Z-scan technology. The nonlinear absorption coefficient β and nonlinear refractive index γ show regular changes from Au to Au/Ag_2Se core/shell nanoparticles. This also caused that their one-photon figures of merit W increase and the two-photon figures of merit T decrease. Finally, the figures of merit $W = 4.15$ and $T = 0.58$ of the Au/Ag_2Se core/shell nanoparticles satisfy the demand of the application of all-optical switch.

topics: nonlinear optics, Z-scan, Au/Ag2Se nanoparticles, FOM

1. Introduction

In recent years, the nanomaterials have attracted much more attention for their multifunction in ultrafast optical information processing [1], all-optical switching [2–7], optical limiter [6, 8–10]. A lot of work has been done [11–16] because of the specific nonlinear optical properties of nanomaterials. The nonlinear optical properties of the nanomaterials are greatly influenced by their size, morphology, and composition [6, 17–20]. For example, the nonlinear absorption coefficient β will decrease with the size of the Au nanoparticles (NPs) increasing. The figures of merit of the Au NPs also have a regular change [17]. The Au nanoparticles and Au nanorods also have different nonlinear absorption and refraction properties [18–20]. Therefore, many different sizes, morphologies and components nanostructures have been prepared and studied [21–24].

In order to characterize the nonlinear optical property of the nanomaterial, there have two parameters which are termed as the figures of merit (FOM). One is one-photon FOM $W = |\gamma|I/\alpha\lambda$ and the other is two-photon FOM $T = \beta\lambda/|\gamma|$, where α and β are the linear and nonlinear absorption coefficient, respectively. The γ is the nonlinear refractive index, λ is the wavelength of the laser and I is the irradiance [3, 7]. The FOM $W > 1$ and $T < 1$ of the materials is essential for applications in all-optical switching. Therefore, the materials will have great potential application in all-optical switching, which require a large nonlinear refractive index and small linear and nonlinear absorption coefficient.

In this paper, we provide an effective method for the preparation of small sized Au NPs and their composite heterostructures. The small-sized Au/Ag_2Se nanoparticles were synthesized in organic environment. This nanostructure has good nonlinear figures of merit. We studied the third-order nonlinear optical properties of the Au NPs and Au/Ag, Au/Ag_2Se core/shell NPs by Z-scan technology. We can effectively control the Au/Ag_2Se core-shell NPs with its average diameter about 8 nm by this method. The Au nanoparticles with average diameter about 5 nm are synthesized in organic environment. With the shell changing from pure Au NPs to Au/Ag_2Se core/shell NPs, the one-photon FOM W is increasing and the two-photon FOM T is decreasing. Finally, $W = 4.15$ and $T = 0.58$ of the Au/Ag_2Se core/shell NPs satisfy the applications of all-optical switching. This is a good all-optical switching nanomaterial.

2. Experimental

2.1. Samples preparation

Au NPs were synthesized in the following steps: 8 ml ethanol, 0.8 ml of oleic acid, and 0.6 g of sodium linoleate were mixed together with stirring. Then, 1.2 ml of gold chloride acid ($HAuCl_4$) aqueous solution (10 mM) was added into the mixed solution and vigorously stirred about 3 min. After

this, 2 ml of ascorbic acid aqueous solution (50 mM) was injected. The color of the solution changed from yellow to purple immediately. Next, 8 ml of cyclohexane was added into solution and stirred for one hour. To extract the Au NPs to cyclohexane, the solution was stored at room temperature for 24 h. The average diameter of the Au became 5 nm. This colloidal solution has a good monodispersion. When the volume of $HAuCl_4$ solution (from 1.2 ml to 3 ml) or the concentration ascorbic acid (from 50 mM to 100 mM) was slightly increased, the diameter of Au NPs was changed from about 4 to 6 nm. This change of diameter was not significant. A slight aggregation began to appear. It seemed that increasing the concentration in a large range would lead to rapid aggregation and precipitation of the samples. Therefore, this method can effectively prepare Au NPs with small size by precise control of the parameters.

Synthesis of Au/Ag core/shell NPs [25] was done in the following way: an amount of 1 ml of toluene containing Au NPs was taken to centrifugate, then the supernatant was removed. The precipitate was dissolved in 6 ml H_2O. Next, 4 ml ethyl glycol (EG), 0.4 ml oleic acid, and 0.3 g sodium linoleate were added into Au NPs solution, and stirring until the solution mixed uniformly. After this, drop by drop of 1 ml $AgNO_3$ (0.3 M) aqueous solution was added with vigorous stirring. Then, 0.6 ml of ascorbic acid (0.2 M) aqueous solution was slowly injected and reacted for 24 h. Finally, to extract the Au/Ag core/shell NPs, 10 ml of toluene was added into the solution. The average diameter of the Au/Ag became about 8 nm.

Au/Ag_2Se core/shell NPs were synthesized as follows [26]: 2 mmol selenium powder, 5 ml oleylamine, and 10 ml oleic acid were mixed together as the Se precursor, next 5 ml Au/Ag colloid was added into it and reacted for 30 min at room temperature. The final product of Au/Ag_2Se was obtained by injecting ethanol and centrifuging at 15000 rpm for 30 min.

2.2. Measurements

Transmission electron microscope (TEM) images were obtained by a JEOL 2010HT microscope. Linear absorbance spectra were recorded on TU-1810 UV-Vis spectrophotometer. The nonlinear optical properties of the samples were measured by using Z-scan technique. The laser pulses used were generated by a mode-locked Ti:sapphire laser (Coherent, Mira 900), operating at a repetition rate of 76 MHz with a pulse duration of 150 fs and a wavelength of 535 nm.

3. Results and discussion

The TEM images of Au NPs, Au/Ag, Au/Ag_2Se core/shell NPs are shown in Fig. 1. We can see that the NPs show a good monodispersity. The average diameters of the Au NPs and Au/Ag core/shell

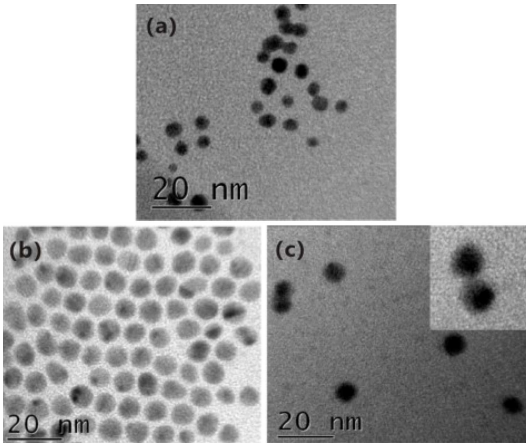

Fig. 1. TEM images of the nanoparticles of Au (a), Au/Ag (b), Au/Ag_2Se (c).

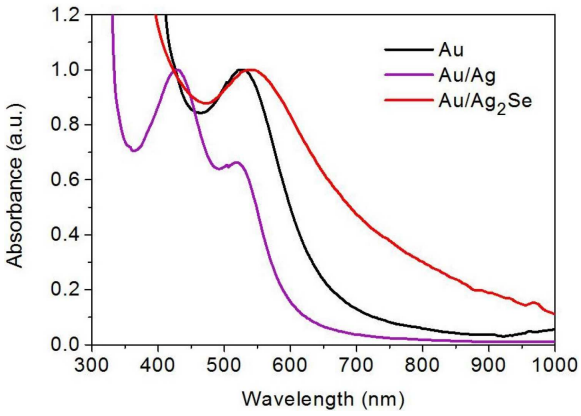

Fig. 2. Linear absorbance spectra of the NPs of Au, Au/Ag, and Au/Ag_2Se. The NPs of Au dissolved in cyclohexane, Au/Ag and Au/Ag_2Se dissolved in toluene.

NPs are approximately 5 nm and 8 nm, respectively. The Au/Ag_2Se core/shell NPs have the approximately same size with Au/Ag NPs, which indicates that the Au/Ag_2Se is generated by oxidation reaction, not the non-epitaxial growth. The core-shell nanostructure can be clearly seen from the illustration at the upper right of Fig. 1c. Therefore, this is an effective method for the preparation of small gold nanoparticles and their composite heterostructures.

The line absorbance spectra of the Au, Au/Ag, and Au/Ag_2Se NPs are shown in Fig. 2. The surface plasmon resonance (SPR) wavelength of the Au NPs is located at 528 nm, and that of Au/Ag core/shell NPs slightly blue-shifted to 526 nm. The peak at 428 nm appears due to a thin layer of Ag shell. The bandwidth of Au/Ag core/shell NPs become slightly narrowed compared to pure Au NPs which is explained as plasmon focusing [27]. In a certain range of scales, the blue-shift will increase with the thickness of Ag shell increasing. The resonance peak of the Au/Ag_2Se core/shell NPs is broaden and slightly red-shifted compared

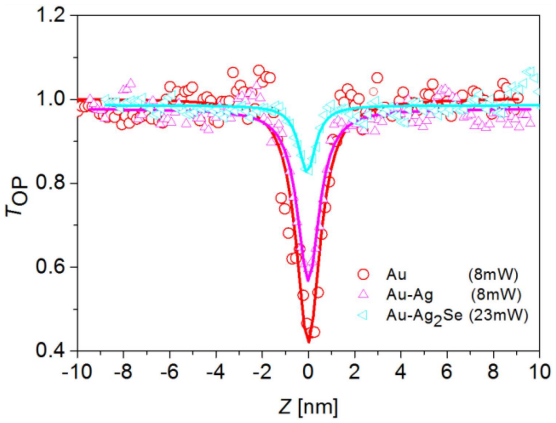

Fig. 3. Nonlinear absorption spectra of the NPs of Au, Au/Ag, and Au/Ag_2Se. The laser pulse excitation wavelength is 535 nm.

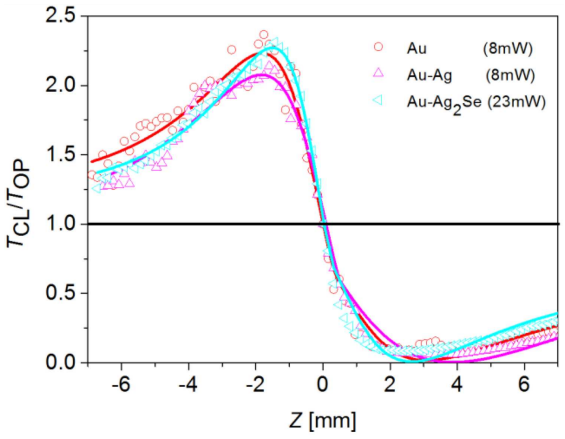

Fig. 4. Normalized closed-aperture Z-scan transmittance divided by the open-aperture of the NPs of Au, Au/Ag, and Au/Ag_2Se. The laser pulse excitation wavelength was 535 nm.

to pure Au NPs due to the change of the surrounding dielectric medium of the Au NPs. This can be explained by the high refractive indices of the silver chalcogenides, which screen the incident electromagnetic field [28].

The nonlinear absorption (NLA) spectrum is measured by using open-aperture Z-scan technique. The normalized transmittance of the open-aperture Z-scan of the NPs can be described using [3]:

$$T_{OP}(z) = \sum_{m=0}^{\infty} \frac{(-q_0)^m}{\left(1+\frac{z^2}{z_0^2}\right)^m (1+m)^{3/2}}, \qquad (1)$$

with

$$q_0 = \beta I_0 L_{\text{eff}}, \quad L_{\text{eff}} = \frac{1}{\alpha}\left[1-\exp(-\alpha L)\right],$$

and where I_0 is the peak irradiance at the focus ($z = 0$), L is the thickness of the sample, and z_0 is the Rayleigh length of the Gaussian incident beam. Figure 3 shows the NLA spectra of the NPs. The laser power to test Au NPs, Au/Ag, and Au/Ag_2Se core/shell NPs were 8 mW and 23 mW, respectively. The NLA coefficient β of the samples can be calculated by fitting the experimental curves. The open-aperture curves have an obvious valley and display a typical reverse-saturable absorption (RSA) feature. It indicates that the NLA coefficient β is positive. The NLA intensity becomes weaker from Au NPs to Au/Ag_2Se core/shell NPs which can be seen from the spectra.

The nonlinear refraction (NLR) is measured by the closed-aperture Z-scan method. The normalized transmittance of the closed-aperture Z-scan of the NPs can be described using [3]:

$$\frac{T_{CL}(z)}{T_{\text{OP}}(z)} = 1 + \frac{4\Delta\phi_0 \frac{z}{z_0}}{\left(\frac{z^2}{z_0^2}+9\right)\left(\frac{z^2}{z_0^2}+1\right)}, \qquad (2)$$

where $\Delta\varphi_0$ relates to the NLR index γ through the expression $\Delta\varphi_0 = \gamma k I_0 L_{\text{eff}}$. Figure 4 shows the close-aperture transmittance normalized $T_{\text{CL}}/T_{\text{OP}}$ as a function of z-position. The Au NPs were dissolved in cyclohexane. The Au/Ag and Au/Ag_2Se core/shell NPs were dissolved in toluene. The peak-valley configuration of the closed-aperture curve indicates the self-defocusing effect of the sample, corresponding to the negative NLR index γ. The NLR index γ also can be obtained by fitting the experimental curves.

TABLE I

The table lists the nonlinear absorption coefficient β, nonlinear refraction index γ, one-photon FOM W and two-photon FOM T of the samples.

	$\beta \times 10^{-9}$ [m/W]	$\gamma \times 10^{-2}$ [cm^2/GW]	W	T
Au	5.10	−1.21	1.59	2.26
Au/Ag	3.91	−1.68	1.82	1.25
Au/Ag_2Se	0.41	−0.38	4.15	0.58

Table I lists the NLA coefficient β, NLR index γ, one-photon figures of merit (FOM) W and two-photon FOM T of the samples. The one-photon FOM W is proportional to the ratio of the NLR index γ and the NLA coefficient β. We can see that the W increases from 1.59 to 4.15 with the Ag_2Se shell formed. The two-photon FOM T is proportional to the ratio of the NLA coefficient β and the NLR index γ. The value of T decreases from 2.26 to 0.58 with the shell changed. The values of W and T of the Au/Ag_2Se satisfy the demand for the application of an all-optical switch. It is a good method to synthesize the material which satisfies the application of the all-optical switch.

4. Conclusion

We provide an effective method for the preparation of small gold nanoparticles and their composite heterostructures. This composite heterostructure has good nonlinear figures of merit. Their linear and nonlinear optical properties have been investigated by UV-vis spectrophotometer and

Z-scan technique, respectively. The one-photon FOM W increases and the two-photon FOM T decreases from Au NPs to Au/Ag_2Se core/shell NPs. The FOM of Au/Ag_2Se core/shell NPs satisfies the demand $W > 1$ and $T < 1$ for the applications of all-optical switching.

Acknowledgments

This work was supported by the National Natural Science Foundation of China (No. 11604180, 11804188, 11904197), and the Science and Technology Plan Projects of Qufu Normal University (No. xkj201522).

References

[1] D. Ricard, P. Roussignol, C. Flytzanis, *Opt. Lett.* **10**, 511 (1985).

[2] G. Lenz, J. Zimmermann, T. Katsufuji, M.E. Lines, H.Y. Hwang, S. Spälter, R.E. Slusher, S.-W. Cheong, *Opt. Lett.* **25**, 254 (2000).

[3] Q.Q. Wang, J.B. Han, H.M. Gong, D.J. Chen, X.J. Zhao, J.Y. Feng, J.J. Ren, *Adv. Funct. Mater.* **16**, 2405 (2006).

[4] N. Kamaraju, S. Kumar, B. Karthikeyan, A. Moravsky, R.O. Loutfy, A.K. Sood, *Appl. Phys. Lett.* **93**, 091903 (2008).

[5] N. Kamaraju, S. Kumar, Y.A. Kim, T. Hayashi, H. Muramatsu, M. Endo, A.K. Sood, *Appl. Phys. Lett.* **95**, 081106 (2009).

[6] Y.H. Lee, Y.L. Yan, L. Polavarapu, Q.H. Xu, *Appl. Phys. Lett.* **95**, 023105 (2009).

[7] K. Wang, H. Long, M. Fu, G. Yang, P.X. Lu, *Opt. Lett.* **35**, 1560 (2010).

[8] A. Patra, N. Venkatram, D. Narayana Rao, T.P. Radhakrishnan, *J. Phys. Chem. C* **112**, 16269 (2008).

[9] C.S.S. Sandeep, A.K. Samal, T. Pradeep, R. Philip, *Chem. Phys. Lett.* **485**, 326 (2010).

[10] M.D. Zidan, Z. Ajji, A.W. Allaf, A. Allahham, *Opt. Laser Technol.* **43**, 1347 (2011).

[11] H.-S. Jun, K.-S. Lee, S.-H. Yoon et al., *Phys. Status Solidi A* **203**, 1211 (2006).

[12] E. Xenogiannopoulou, P. Aloukos, S. Couris, E. Kaminska, A. Piotrowska, E. Dynowska, *Opt. Commun.* **275**, 217 (2007).

[13] E. Xenogiannopoulou, K. Iliopoulos, S. Couris, T. Karakouz, A. Vaskevich, I. Rubinstein, *Adv. Funct. Mater.* **18**, 1281 (2008).

[14] K. Iliopoulos, D. Athanasiou, A. Meristoudi, N. Vainos, S. Pispas, S. Couris, *Phys. Status Solidi A* **205**, 2635 (2008).

[15] A. Azhagu Parvathi, A. John Peter, *Acta Phys. Pol. A* **124**, 706 (2013).

[16] V. Singh, P. Aghamkar, B. Lal, *Acta Phys. Pol. A* **123**, 39 (2013).

[17] K. Wang, H. Long, M. Fu, G. Yang, P.X. Lu, *Opt. Express* **18**, 13874 (2010).

[18] J.T. Seo, Q. Yang, W.-J. Kim et al., *Opt. Lett.* **34**, 307 (2009).

[19] J.Z. Dong, X.L. Zhang, Y.A. Cao, W.S. Yang, J.G. Tian, *Mater. Lett.* **65**, 2665 (2011).

[20] X.L. Liu, F. Nan, Y.H. Qiu, D.J. Yang, S.J. Ding, Q.Q. Wang, *J. Phys. Chem. C* **122**, 3958 (2018).

[21] J. Zhu, S.N. Wang, J.J. Li, J.W. Zhao, *J. Lumin.* **199**, 216 (2018).

[22] S. Bhagyaraj, S. Perumbilavil, R. Udayabashkar, R.V. Mangalaraja, S. Thomas, N. Kalarikkal, O.S. Oluwafemi, *Phys. Chem. Chem. Phys.* **21**, 11424 (2019).

[23] J. Yang, J.Y. Ying, *J. Am. Chem. Soc.* **132**, 2114 (2010).

[24] A. Chafai, I. Essaoudi, A. Ainane, R. Ahuja, *Results Phys.* **14**, 102414 (2019).

[25] J.T. Zhang, Y. Tang, L. Weng, M. Ouyang, *Nano Lett.* **9**, 4061 (2009).

[26] J.T. Zhang, Y. Tang, K. Lee, M. Ouyang, *Science* **327**, 1634 (2010).

[27] J. Becker, I. Zins, A. Jakab, Y. Khalavka, O. Schubert, C. Sönnichsen, *Nano Lett.* **8**, 1719 (2008).

[28] M. Liu, P. Guyot-Sionnest, *J. Mater. Chem.* **16**, 3942 (2006).